CHAPTER-VII

Exploration of Miscellaneous Interfaces of a Green Liquid in Diverse Solvent Systems by the Process of Physicochemical Contrivances

VII.1. INTRODUCTION

Ionic liquids have unique intrinsic properties, such as negligible vapour pressure, large liquid range, ability of dissolving a variety of chemicals, high thermal stability, large electrochemical window and their potential as 'designer solvents' and 'green' replacements for volatile organic solvents[1-3] used in reactions involving inorganic and bio-catalysis etc. They are also utilized as heat transfer fluids for processing biomass and as electrically conductive liquids in electrochemistry (batteries and solar cells) [4-6]. In the modern technology, the application of the salt is well understood by studying the ionic solvation or ion association. Ionic association of electrolytes in solution depends on the mode of solvation of its ions [7-10] which in turn depends on the nature of the solvent/solvent mixtures. Such solvent properties as viscosity and the relative permittivity have been taken into consideration as these properties help in determining the extent of ion association and the solvent-solvent interactions. The non-aqueous system has been of immense importance [11,12] to the technologist and theoretician as many chemical processes occur in these systems. The volumetric, viscometric and interferometric behavior of solutes has been found to be very useful in elucidating the various interactions occurring in solutions. Studies on the effect of concentration (molarity), the apparent molar volumes of solutes have been extensively studied to obtain information on ion-ion, ion -solvent and solvent-solvent interactions [13-17].

In view of the above and in continuation of our studies, we have performed a systematic study on the conductance, density, viscosity, refractive index, ultrasonic

Published in I. J. Adv. Chem. Sci. 56 (2014) 253-263

speed and FTIR study of 1-butyl-1-methylpyrrolidium bromide [BMP][Br] in pure formamide (FA), N, N-dimethyl formamide (DMF) and N, N-dimethyl acetamide (DMA) at 298.15 K and we have attempted to report the limiting molar conductance (Λ_o), the association constant (K_A), the association diameter (R) and Walden product for ion-pair formation. Also the limiting apparent molar volume (ϕ_V^0), viscosity B-coefficients, molar refraction (R_M) and limiting apparent molar adiabatic compressibility (ϕ_K^0) for the [BMP][Br] in the same solvent systems.

VII.2. EXPERIMENTAL SECTION

VII.2.1. Materials

1-butyl-1-methylpyrrolidium bromide [BMP][Br] of puriss grade was procured from Sigma-Aldrich, Germany and was used as purchased. The mass fraction purity of the IL has ≥ 0.99. Formamide (≥98.5%) and DMF (≥99.5%) were obtained from Sd. Fine Chemicals, India. and DMA (≥99.5%) has obtained from Thomas Beaker, India. The solvents were purified using standard methods. [18]

VII.2.2. Apparatus and Procedure

The conductance measurement was carried out in a Systronic-308 conductivity meter (accuracy ± 0.01 %) using a dip-type immersion conductivity cell, CD-10, having a cell constant of approximately 0.1 ± 0.001 cm^{-1}. Measurement was made in a water bath maintained within T = 298.15 ± 0.01 K and the cell was calibrated by the method proposed by Lind et al. [19] The conductance data were reported at a frequency of 1 kHz and the accuracy was ±0.3%.

Stock solutions for the IL in three different solvents were prepared by mass (Mettler Toledo AG285 with uncertainty 0.0003 g), and the working solutions were obtained by mass dilution at 298.15K. The uncertainty of molarity of different solutions was evaluated to ±0.0001 mol dm^{-3}. The density (ρ) was measured by means of vibrating-tube Anton Paar density-meter (DMA 4500M) with a precision of 0.0005 $g \cdot cm^{-3}$. It was calibrated by double-distilled water and dry air.

The viscosity was measured with the help Brookfield DV-III Ultra Programmable Rheometer with spindle size-42 fitted to a Brookfield Digital Bath TC-500.

The refractive index was also measured with the help Refractive index was measured with the help of a Digital Refractometer Mettler Toledo. The light source was LED, k= 589.3 nm. The refractometer was calibrated twice using distilled water, and calibration was checked after every few measurements. The uncertainty of refractive index measurement was ±0.0002 units.

The ultrasonic velocities, u (ms^{-1}) were determined using an ultrasonic interferometer (Model M-83) from Mittal enterprises. The interferometer working at 2 MHz is based on the same principle as was used by Freyer et al. [20] and Kiyoharo et al. [21,22] The obtained velocities were corrected for diffraction errors as given by Subrahmayan et al. [23]. The maximum uncertainty in the velocity is ±0.5 m s^{-1}. The temperature was controlled within ±0.01 K using a Lauda thermostat for velocity measurements.

Infrared spectra were recorded in 8300 FT-IR spectrometer (Shimadzu, Japan). The details of the instrument have already been previously described [24].

VII.3. RESULTS AND DISCUSSION

VII.3.1. Conductance calculation

The solvent properties have been given in Table VII.1. The molar conductances (Λ) with corresponding concentrations of [BMP][Br] in FA, DMA and DMF have been given in Table VII.2. Linear conductimetric curves (Λ versus $\sqrt{c}$) have been obtained and extrapolation of $\sqrt{c}$ = 0 evaluated the starting limiting molar conductance for the electrolyte. The conductance data for ion-pair formation have been analyzed using the Fuoss conductance equation [14]. For a given set of conductivity values (c_j, Λ_j; j = 1…….n), three adjustable parameters, i.e., Λ_0, K_A and R have been derived from the Fuoss equation. Here, Λ_0 is the limiting molar conductance, K_A is the observed association constant and R is the association distance, i.e., the maximum centre to centre distance between the ions in the solvent separated ion-pairs. There is no precise

method [25] for determining the R value but in order to treat the data in our system, R value is assumed to be, $R = a + d$, where a is the sum of the crystallographic radii of the ions and d is the average distance corresponding to the side of a cell occupied by a solvent molecule. The distance, d, is given by:

$$d = 1.183 \left(M / \rho\right)^{1/3} \quad (1)$$

where M is the molar mass and ρ is the density of the solvent.

The Fuoss conductance equation may be represented as follows:

$$\Lambda = P\Lambda_o[(1+R_X)+E_L] \quad (2)$$

$$P = 1-\alpha(1-\gamma) \quad (3)$$

$$\gamma = 1-K_A c\gamma^2 f^2 \quad (4)$$

$$-\ln f = \beta\kappa / 2(1+\kappa R) \quad (5)$$

$$\beta = e^2 / \left(\varepsilon_r k_B T\right) \quad (6)$$

$$K_A = K_R / (1-\alpha) = K_R / (1+K_S) \quad (7)$$

here, Λ_0 is the limiting molar conductance, K_A is the observed association constant, R is the association distance, R_X is the relaxation field effect, E_L is the electrophoretic counter current, k is the radius of the ion atmosphere, ε_r is the relative permittivity of the solvent mixture, e is the electron charge, c is the molarity of the solution, k_B is the Boltzmann constant, K_S is the association constant of the contact-pairs, K_R is the association constant of the solvent-separated pairs, γ is the fraction of solute present as unpaired ion, α is the fraction of contact pairs, f is the activity coefficient, T is the absolute temperature and β is twice the Bjerrum distance.

The computations were performed using the program suggested by Fuoss [14]. The initial Λ_0 values for the iteration procedure are obtained from Shedlovsky extrapolation of the data [26]. Input for the program is the number of data, n, followed by ε_r, η (viscosity of the solvent mixture), initial Λ_0 value, T, ρ (density of the solvent mixture), mole fraction of the first component, molar masses, M_1 and M_2 along with c_j, Λ_j values where j = 1, 2…….n and an instruction to cover preselected range of R values.

In practice, calculations are performed by finding the values of Λ_0 and α which minimize the standard deviation, δ, whereby

$$\delta^2 = \sum [\Lambda_j(cal) - \Lambda_j(obs)]^2 / (n-m) \quad (8)$$

for a sequence of R values and then plotting δ against R, the best- fit R corresponds to the minimum of the δ–R versus R curve. So, an approximate sum is made over a fairly wide range of R values using 0.1 increment to locate the minimum but no significant minima is found in the δ - R curves. Finally, the corresponding Λ_0 and K_A values have been obtained which are reported in Table VII.3 along with R and δ for the all the solutions.

A perusal of Table VII.3 and Figure VII.1 shows that the limiting molar conductance (Λ_0) of all the electrolytes studied is highest in case of DMF and lowest in case of FA among the studied solvents. The trend of Λ_0 fof the electrolyte in three different solvents is as follows:

DMF > DMA > FA

The more number of molecules interacting have been lead with the help greater ion-solvation. It has been seen that in case of FA, the K_A value are greater (Table VII.3), which obviously made the same inference that ion-solvent as well as ion-association is higher in FA. Similarly, the lower K_A value for DMF, suggesting the weakest ion-solvent interaction, is in lowest viscous solvent.

The Gibbs energy change of solvation, ΔG^o, is determined by the following equation [27] and reported in Table VII.4.

$$\Delta G^o = -RTlnK_A \quad (9)$$

The negative values of ΔG^o can be explained by considering the participation of specific electrostatic interaction in the ion-association process [30]. The negative in ΔG^o values have states that the ion-solvent interaction is more feasible in these solution systems. The decrease in the value of ΔG^o, from DMF to FA, provides the spontaneity of the ion-solvent interactions, which have been trends from DMF to FA, as a results ion-association increases. This result indicates the extent of solvation enhanced by the following order:

DMF < DMA < FA

The observed ion-solvent interactions can be explain as follow: In case of (IL+FA) binary solution, the positively charged N atom of $[BMP]^+$ may interacts with more negative oxygen atom of FA. Again, negatively charged Br^- ion of IL interacts with positively charged N atom of resonance structure of formamide (Scheme VII.1). In DMA electrophilic character of N atom reduced due to presence of two $-CH_3$ groups, which exhibit +I affect. So, interaction between Br^- of IL and N atom of DMA decreases. On the other hand one $-CH_3$ is attached with C=O group present in DMA, which, increases the nucleophilic character of oxygen and the interaction between N atom of $[BMP]^+$ and oxygen atom of DMA increases. But, in DMF electrophilic nature of N atom decreases due to +I effect of $-CH_3$ groups, therefore, interaction between Br^- and N atom of DMF decreases. Once again, there is no mesmerizing power in DMA, i.e., interaction mode of oxygen atom of DMF and N of $[BMP]^+$ are lower (Scheme VII.1).

The ionic level of interaction has been interpreted from the results of ionic contribution of electrolyte. The starting point for most evaluations of ionic conductance is Stokes' law which states that the limiting Walden product ($\lambda_o^{\pm}\eta$), (the limiting ionic conductance-solvent viscosity product) for any singly charged, spherical ion is a function only of the ionic radius and thus, under normal conditions, is a constant. The ionic conductances $\lambda_o^{\pm}$ for the cation $[BMP]^+$ and the anion Br^- in all the solvents were calculated using tetrabutylammonium tetraphenylborate (Bu_4NBPh_4) as a 'reference electrolyte' following the scheme as suggested by B. Das et al. [28] The ionic limiting molar conductances $\lambda_o^{\pm}$ for $[BMP]^+$ and Br^- in all the solvents have been calculated by interpolation of conductance data from the literature [29] using cubic spline fitting. The $\lambda_o^{\pm}$ values were in turn utilized for the calculation of Stokes' radii (r_s**)** according to the classical expression [30]

$$r_S = \frac{F^2}{6\pi N_A \lambda_o^{\pm} r_c} \qquad (10)$$

where, r_c is the crystallographic radii, N_A is the Avogadro number, and F is the Faraday constant. The values of ionic limiting molar conductance $\lambda^{\pm}_o$, ionic Walden product $\lambda_o^{\pm}\eta$, Stokes' radii r_s, and crystallographic radii r_c are presented in Table VII.5. A perusal of table VII.5 shows the ionic conductance of cation $[BMP]^+$ and anion Br^- is lower in case

of FA, compared to other two solvents, suggests that the ion-solvent interactions as well as ion-solvation of the individual ions are higher. Similar relation has been observed from Stokes' radii (r_s) for both cation and anion, are higher in FA than DMA, which is in term higher than DMF; the results also indicate the higher salvation in FA than other two. The r_s value of cation $[BMP]^+$ is higher for anion Br^-, which results ion-solvation (ion-solvent interaction) is higher for $[BMP]^+$ ion than Br^- in all investigated solvents.

VII.3.2. Density calculation

The measured values of densities of [BMP][Br] in FA, DMA and DMF at 298.15 K are listed in Table VII.6. The densities and viscosities of the electrolytes in different solvents increase linearly with the concentration at the studied temperature. For this purpose, the apparent molar volumes ϕ_V given in Table VII.9 were determined from the solution densities using the following equation [31]

$$\phi_V = M/\rho_o - 1000(\rho - \rho_o)/c\rho_o \quad (11)$$

where M is the molar mass of the solute, c is the molarity of the solution, ρ and ρ_0 are the densities of the solution and solvent, respectively. The limiting apparent molar volumes ϕ_V^0 were calculated using a least-squares treatment to the plots of ϕ_V versus $\sqrt{c}$ using the following Masson equation [32].

$$\phi_V = \phi_V^0 + S_V^* \cdot \sqrt{c} \quad (12)$$

where ϕ_V^0 is the limiting apparent molar volume at infinite dilution and S_V^* is the experimental slope.

The plots of ϕ_V against the square root of the molar concentration $\sqrt{c}$ were found to be linear with negative slopes. The values of ϕ_V^0 and S_V^* are reported in Table VII.6. The variation of ϕ_V^0 for this electrolyte with the solvents is shown in Figure VII.2. From Table VII.6 it is observed that ϕ_V^0 values for this electrolyte are generally positive for all the solvents and is highest in case of [BMP][Br] in FA. This indicates the presence

of strong ion–solvent interactions and the extent of interactions increases from DMF to FA.

On the contrary, the S_V^* indicates the extent of ion-ion interaction. The values of S_V^* shows that the extent of ion-ion interaction is highest in case of DMF and is lowest in FA. Owing to a quantitative comparison, the magnitude of ϕ_V^0 are much greater than S_V^*, in every solutions. This suggests that ion-solvent interactions dominate over ion-ion interactions in all the solutions. The values of ϕ_V^0 also support the fact that higher ion-solvent interaction in FA, leads to lower conductance of [BMP][Br] in it than DMA and DMF, discussed earlier.

VII.3.3. Viscosity calculation

Another transport property of the solution is viscosity has been studied for comparison and conformation of the solvation of the electrolyte in the chosen solvents. The viscosity data has been analyzed using Jones-Dole equation [33].

$$(\eta/\eta_0 - 1)/\sqrt{c} = A + B\sqrt{c} \qquad (13)$$

where η and η_0 are the viscosities of the solution and solvent respectively. The values of *A*-coefficient and *B*-coefficient are obtained from the straight line by plotting $(\eta/\eta_0 - 1)/\sqrt{c}$ against $\sqrt{c}$ which are reported in Table VII.7.

The effects of ion-solvent interactions on the [BMP][Br] solution in FA, DMA and DMF viscosity can be inferred from the *B*-coefficient [34, 35]. The viscosity *B*-coefficient is a valuable tool to provide information concerning the solvation of the solutes and their effects on the structure of the solvent. From Table VII.7 and Figure VII.3 it is evident that the values of the *B*-coefficient are positive, thereby suggesting the presence of strong ion-solvent interactions, and strengthened with an increase the solvent viscosity value, are agreement with the results obtained from ϕ_V^0 values discussed earlier. An assessment of Table VII.7 and Figure VII.3 shows that the values of the *A*-coefficient are very small for the solutions under investigation at all solvents indicating

the presence of weak ion–ion interactions, and these interactions further decrease from FA to DMF. This shows that with the increase in the viscosity *B*-coefficient of the solvent the mobility of the ions of the solvated IL decrease and hence the conductance also decreases. That is why, [BMP][Br] is more solvated in DMF than the other two solvents. Thus, the trend of ion-solvent interaction is FA >DMA>DMF. The viscosity *A*- and *B*-coefficients are in excellent agreement with the results drawn from the volumetric studies.

VII.3.4. Refractive index calculation

The molar refraction, R_M can be evaluated from Lorentz-Lorenz relation [36]

$$R_M = \{(n_D^2-1)/ (n_D^2+2)\}(M/\rho) \quad (14)$$

where R_M, n_D, M and ρ are the molar refraction, refractive index, molar mass and density of solution respectively. The refractive index of a compound describes its ability to refract light as it moves from one medium to another and thus, the higher the refractive index of a compound, the more the light is refracted. As stated by Deetlefs *et al*.[37] the refractive index of a substance is higher when its molecules are more tightly packed or in general when the compound is denser. Hence a perusal of Table VII.8 and Figure VII.4 shows that the refractive indices (n_D) and molar refractions (R_M) of all the electrolytes (0.05M) are highest in FA and lowest in case of DMF among the three solvents. The trend of n_D and R_M of the three ionic liquids in three different solvents is as follows:

FA>DMA>DMF

As R_M, is directly proportional to molecular polarizability, it is evident from Table VII.8 and Figure VII.4 that the overall polarizabilty of all the electrolytes is highest in case of FA in comparison to the other solvents. It is also found that the refractive index (n_D) and molar refraction (R_M) of [BMP][Br] is highest in FA. So, according to the statement of Deetlefs *et al.* it is concluded that the molecules of [BMP][Br] are most tightly packed among in FA. The packing is least in the case of DMF.

VII.3.5. Ultrasonic speed calculation

The adiabatic compressibility (β) was evaluated from the following equation:

$$\beta = 1/u^2 \rho \qquad (15)$$

[16].

$$\phi_K = M\beta / \rho + 1000\left(\beta\ \rho_o - \beta_o \rho\right)\ / c\rho\ \rho_o \qquad (16)$$

where M is the molar mass and β_0, β are the adiabatic compressibility of the solvent and solution respectively and c is the molarity of the solution. Limiting partial molar adiabatic compressibilities (ϕ_K^0) and experimental slopes (S_K^*) were obtained by fitting ϕ_K against the square root of molarity of the electrolyte ($\sqrt{c}$) using the method of least squares.

$$\phi_K = \phi_K^0 + S_K^* . \sqrt{c} \qquad (17)$$

The values of ϕ_K^0 and S_K^* are presented in Table VII.9. Since the values of ϕ_K^0 and S_K^* are measures of solute-solvent and solute-solute interactions respectively, a perusal of Table VII.9 shows that the ϕ_K^0 values are in good agreement with those drawn from the values of ϕ_V^0 discussed earlier.

Acoustic relaxation time (τ) [38] is obtained using the relation:

$$\tau = \left(\frac{4\eta}{3\rho u^2} \right) \qquad (18)$$

Relaxation time is the time taken for the excitation energy to appear as translational energy. The increase in acoustic relaxation time with concentration of solute suggests interactions among the components of solution. In the present case from Table VII.9 relaxation time increases with increase in concentration of IL. The increase of relaxation time indicates the presence of molecular interaction in the mixture and the order is FA >DMA>DMF.

The schematic representation of ion-solvation, for the particular ion in the studied solvents, in view of various derived parameters is depicted in Scheme VII.2**.**

VII.3.6. FT-IR calculation

With the help of FT-IR spectroscopy the molecular interactions existing between the solute and the solvents have been studied. At first the IR spectra of the pure solvents were studied. The stretching frequencies of the key groups are given in Table VII.10.

The FT-IR spectra of the ionic liquid in FA show that the peak for C=O at 1755cm^{-1} shifts to 1785.2 cm^{-1} for [BMP][Br] respectively due to the disruption of strong H-bonding [40] interaction in FA molecules leading to the formation of ion-dipole interaction between [BMP]$^{+}$ and C=O dipole.

Similar types of interactions are observed in case of DMA where the sharp peak for C=O shifts from 1672 cm^{-1} to 1695.4 cm^{-1}. In this case the shifting is due to ion-dipole interaction between [BMP] $^{+}$ and C=O dipole.

In case of DMF a sharp peak is obtained at 1654 cm^{-1} for C=O which shifts to 1675 cm^{-1}, on addition of the electrolyte [BMP][Br], due to the interaction of [BMP]$^{+}$ with the C=O dipole showing ion-dipole interaction which is obviously responsible the disruption of H-bonding interaction in DMF molecules [41].

VII.4. CONCLUSION

The extensive conductometric study of [BMP][Br] in FA, DMA, and DMF leads the conclusion that the electrolyte more associated in FA than in the other two solvents. The reliable value of volumetric, viscometric and interferometric studies also intends to map the physicochemical behaviour in solution and suggests that in solution there is more ion–solvent interaction than ion–ion interaction. The molar refraction values also support the above fact that the highest ion-solvent interaction is seen in case of FA solvent. In all the solvents the electrolyte forms ion-dipole interactions as evident from the FT- IR studies.

TABLES

Table VII.1: Density (ρ), viscosity (η), refractive index (n_D), ultrasonic speed (u) and relative permittivity (ε) of the different solvents FA, DMA and DMF.

Solvents	$\rho \cdot 10^{-3}$/kg m^{-3}	η/mPa s	n_D	u/ms^{-1}	E
FA	1.12110[39]	3.23[39]	1.4459[39]	1582.96[40]	110.21[42]
DMA	0.93660[41]	1.95[41]	1.4375[43]	1463.00[41]	38.60[42]
DMF	0.94430[41]	0.92[41]	1.4305[43]	1465.00[41]	36.71[42]

Table VII.2: Concentration (c) and molar conductance (Λ) of [BMP][Br] in Formamide, DMA and DMF at 298.15 K.

$c \cdot 10^4$/ mol·dm^{-3}	$\Lambda \cdot 10^4$/ S·m^2·mol^{-1}	$c \cdot 10^4$/ mol·dm^{-3}	$\Lambda \cdot 10^4$/ S·m^2·mol^{-1}	$c \cdot 10^4$/ mol·dm^{-3}	$\Lambda \cdot 10^4$/ S·m^2·mol^{-1}
[BMP][Br]					
Formamide		DMA		DMF	
0.6889	14.80	0.7056	40.70	0.7569	48.80
1.5625	14.40	1.8769	39.55	1.7956	47.70
2.6896	14.01	3.8809	38.50	3.0276	46.90
4.4521	13.67	6.1504	38.00	4.7524	45.80
5.8564	13.13	8.5849	37.00	7.1824	44.70
7.7284	12.92	12.0409	35.80	10.5625	43.60
9.4249	12.66	16.1604	34.80	14.2129	42.50
11.9025	12.33	19.0969	34.20	17.4724	41.50
14.8225	12.11	22.2784	33.10	20.4304	41.20
18.7489	11.95	25.2004	32.70	24.1081	40.40
21.6225	11.62	28.1961	32.04	28.6225	39.30
24.6016	11.31	30.8025	31.95	32.9476	38.70

29.0521	10.80	34.4569	31.05	37.0881	38.20
35.4025	10.40	40.0689	30.00	41.9904	37.60
42.7716	10.00	44.3556	29.30	45.6976	37.40

Table VII.3: Limiting molar conductance (Λ_o), association constant (K_A), co-sphere diameter (R) and standard deviations of experimental Λ (δ) obtained from Fuoss conductance equation for [BMP][Br] in Formamide, DMA and DMF at 298.15 K.

Solvent	$\Lambda_o \cdot 10^4$/S·m^2·mol^{-1}	K_A/ dm^3·mol^{-1}	R/Å	δ
		[BMP][Br]		
Formamide	14.66	169.83	22.57	0.18
DMA	40.94	138.64	43.51	0.20
DMF	48.56	109.08	37.27	0.45

Table VII.4: Walden product ($\Lambda_o \cdot \eta$) and Gibb's energy change (ΔG°) of [BMP][Br] in Formamide, DMA and DMF at 298.15 K.

Solvents	$\Lambda_o \cdot \eta \cdot 10^4$/ S·m^2·mol^{-1}mPa	$10^3 \Delta G^\circ$/ kJ·mol^{-1}
	[BMP][Br]	
Formamide	47.35	-12.73
DMA	80.08	-12.26
DMF	44.68	-11.63

Table VII.5: Limiting Ionic Conductance ($\lambda_0^{\pm}$), Ionic Walden Product ($\lambda_0^{\pm}\eta$), Stokes' Radii (r_s), and Crystallographic Radii (r_c) of [BMP][Br] in Formamide, DMA and DMF at 298.15 K.

Solvent	ion	$\lambda_0^{\pm}$ (S·m²·mol⁻¹)	$\lambda_0^{\pm}\eta$ (S·m²·mol⁻¹mPa)	r_s (Å)	r_c(Å)
Formamide	$[BMP]^+$	3.06	9.87	8.30	5.05
	Br^-	11.60	37.48	2.19	1.33
DMA	$[BMP]^+$	8.53	16.73	4.90	5.05
	Br^-	32.41	63.51	1.29	1.33
DMF	$[BMP]^+$	10.12	9.31	8.80	5.05
	Br^-	38.44	35.36	2.32	1.33

Table VII.6: Concentration (c), density (ρ), apparent molar volume (ϕ_V), limiting apparent molar volume (ϕ_V^0) and experimental slope (S_V^*) for [BMP][Br] in Formamide, DMA and DMF at 298.15K and Experimental Pressure 0.1MPa.

Solvents	c/ mol·dm^{-3}	$\rho\cdot10^{-3}$/ kg m^{-3}	$\phi_V\cdot10^6$/ m^3·mol^{-1}	$\phi_V^0\cdot10^6$/ m^3·mol^{-1}	$S_V^*\cdot10^6$/ m^3 · mol$^{-3/2}$ ·dm$^{3/2}$
			[BMP][Br]		
Formamide	0.005	1.13305	170.0	207.3	-541.0
	0.020	1.14312	130.0		
	0.035	1.15207	105.5		
	0.050	1.16055	86.4		
	0.065	1.16928	68.0		
	0.080	1.17679	56.0		
DMA	0.005	0.94410	114.0	139.2	-341.3
	0.020	0.95192	97.0		
	0.035	0.96035	81.4		

	0.050	0.96904	67.0		
	0.065	0.97950	52.0		
	0.080	0.98715	42		
DMF	0.005	0.95849	69.9	83.2	-193.4
	0.020	0.96695	60.0		
	0.035	0.97400	52.6		
	0.050	0.98228	45.2		
	0.065	0.99158	37.0		
	0.080	1.00223	28.8		

Table VII.7: Concentration (*c*) viscosity (η), $\frac{(\eta_r - 1)}{\sqrt{c}}$, viscosity *A* and *B* coefficients for [BMP][Br] in Formamide, DMA and DMF at 298.15K and Experimental Pressure 0.1MPa.

Solvents	c /mol·dm^{-3}	η/mPa·s	$\frac{(\eta_r - 1)}{\sqrt{c}}$	B /dm^3·mol^{-1}	A /dm$^{3/2}$·mol$^{-1/2}$
		[BMP][Br]			
Formamide	0.005	3.24	0.026	0.304	0.0038
	0.020	3.25	0.047		
	0.035	3.26	0.061		
	0.050	3.28	0.072		
	0.065	3.29	0.080		
	0.080	3.31	0.088		
DMA	0.005	1.95	0.020	0.226	0.0042
	0.020	1.96	0.037		
	0.035	1.97	0.047		
	0.050	1.98	0.055		
	0.065	1.98	0.062		
	0.080	1.99	0.068		

DMF	0.005	0.94	0.016	0.161	0.0045
	0.020	0.94	0.027		
	0.035	0.95	0.034		
	0.050	0.95	0.041		
	0.065	0.96	0.046		
	0.080	0.96	0.050		

Table VII.8: Refractive indices (n_D) and molar refractions (R_M) of [BMP][Br] in Formamide, DMA and DMF at Temperature (^{n} T) 298.15K and Experimental Pressure 0.1MPa.

Solvents	n_D	R_M/m^3·mol^{-1}
	[BMP][Br]	
Formamide	1.5389	61.616
	1.5399	61.625
	1.5412	61.632
	1.5471	61.637
	1.5499	61.641
	1.5501	61.645
DMA	1.4376	61.269
	1.4377	61.289
	1.4379	61.295
	1.4381	61.314
	1.4383	61.327
	1.4383	61.333
DMF	1.4310	60.943
	1.4314	60.960
	1.4315	60.969
	1.4315	60.975
	1.4317	60.991
	1.4318	61.010

Table VII.9: Limiting partial adiabatic compressibility (ϕ_K^0) and experimental slope (S_K^*) of [BMP][Br] in Formamide, DMA and DMF at Temperature (^{n} *T*) 298.15K and Experimental Pressure 0.1MPa.

Solvents	ϕ_K^0 x 10^{10} ($m^3\ mol^{-1}\ Pa^{-1}$)	S_K^* x 10^4 ($m^3\ mol^{-3/2}\ Pa^{-1}\ kg^{1/2}$)	τ x 10^{-6} (Sec)
	[BMP][Br]		
Formamide	0.11	-0.98	12.17
DMA	0.01	-0.76	5.21
DMF	-0.08	-0.56	2.50

Table VII.10: Stretching frequencies of the functional groups present in the pure solvent and change of frequency after addition of 0.05(M) concentration of [BMP][Br] in Formamide, DMA and DMF.

Solvents	Stretching frequencies(cm^{-1})	
	Pure Solvent	Solvent + [BMP] Br
Formamide	C=O (1755)	C=O (1785.2)
DMA	C=O (1672)	C=O (1695.4)
DMF	C=O (1654)	C=O (1675.0)

FIGURES

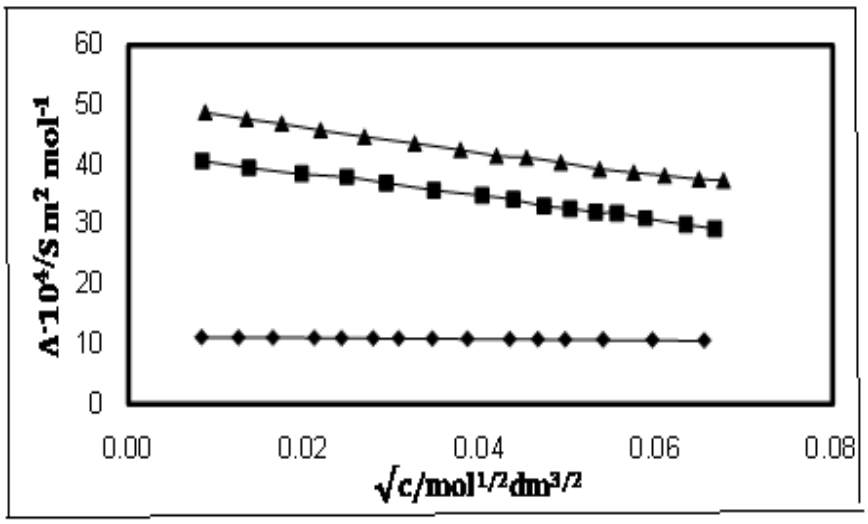

Figure VII.1: Plot of $\sqrt{c}$ versus molar conductance (Λ) for [BMP][Br] in Formamide (—♦—) , DMA (—■—) and DMF (—▲ —) at 298.15 K.

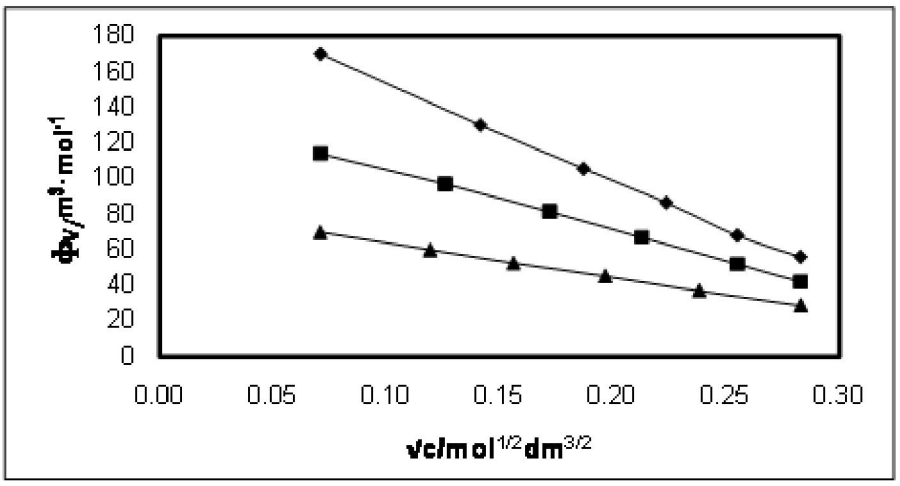

Figure VII.2: Plot of $\sqrt{c}$ versus Limiting apparent molar volume (ϕ_V^0) for [BMP][Br] in Formamide (—♦—), DMA (—■—) and DMF (—▲ —) at 298.15 K.

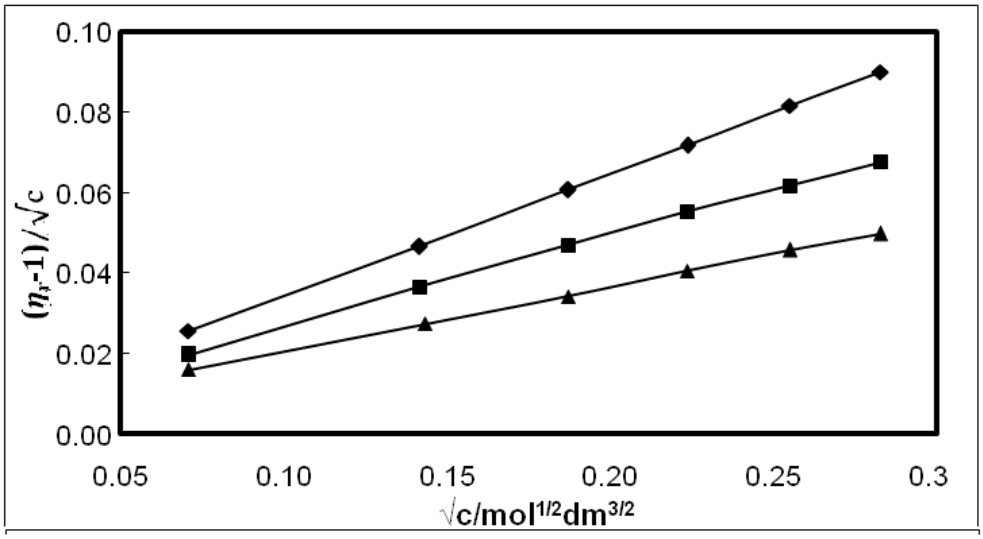

Figure VII.3: Plot of √c vs $\frac{(\eta_r - 1)}{\sqrt{c}}$ for [BMP][Br] in Formamide (—♦—) , DMA(—■—) and DMF (—▲ —) at 298.15 K.

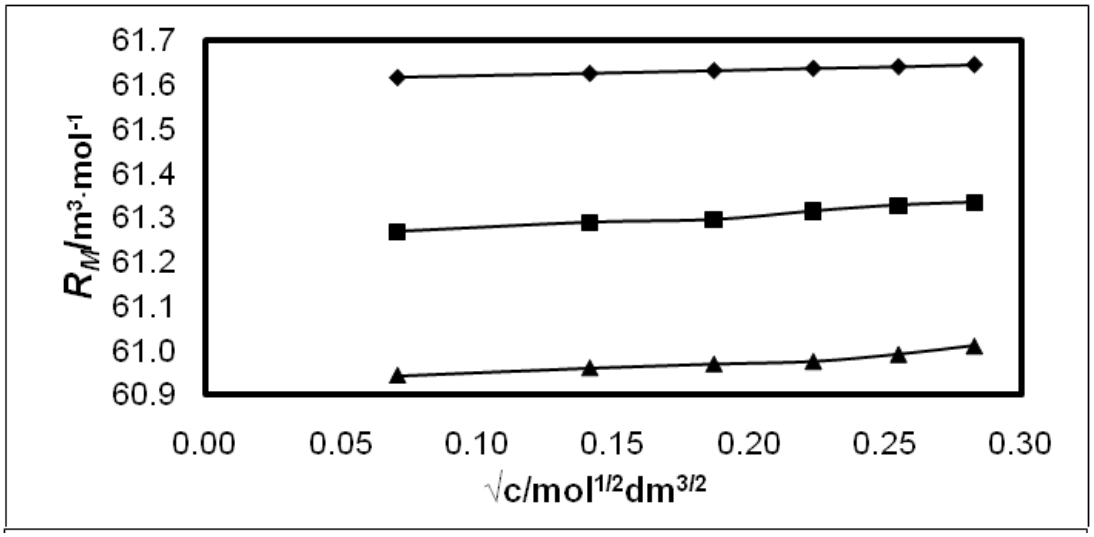

Figure VII.4: Plot of √c versus R_M for [BMP][Br] in Formamide (—♦—) , DMA(—■—) and DMF (—▲ —) at 298.15 K.

SCHEMES

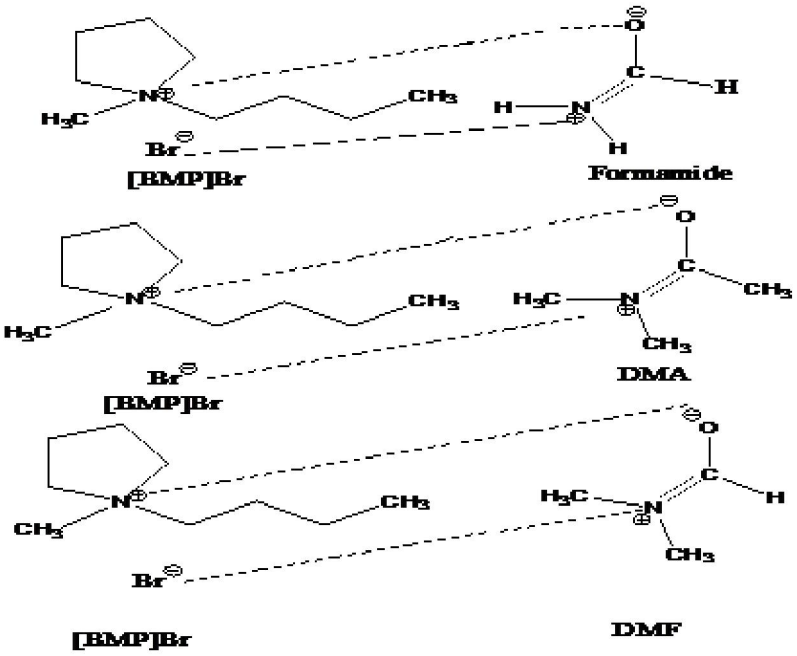

Scheme VII.1. Phase of interaction between [BMP]Br and Formamide, DMA and DMF respectively.

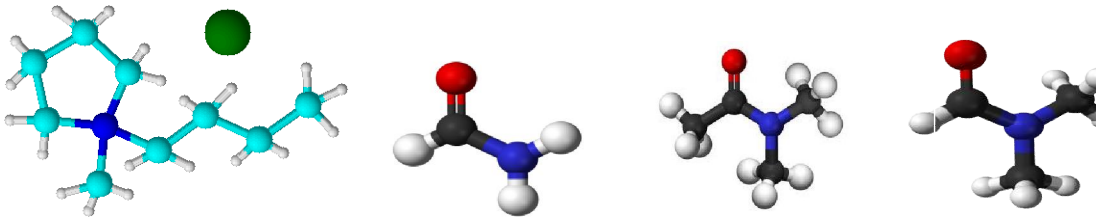

1-butyl-1-methylpyrrolidium bromide | Formamide | DMA | DMF

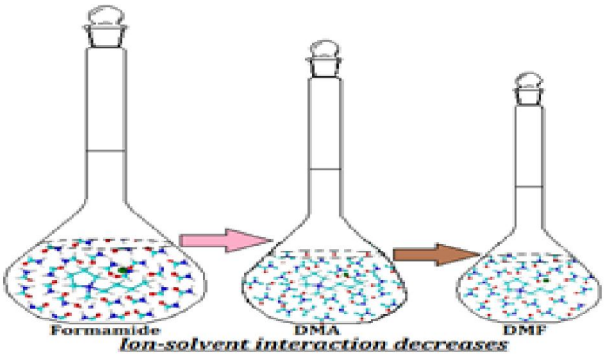

Scheme VII.2. Trend of Ion-solvent interaction between [BMP]Br and Formamide, DMA and DMF respectively.